MATHEMATICAL BIOSCIENCES
AND ENGINEERING
Volume **3**, Number **3**, July **2006**

http://www.mbejournal.org/

pp. **527–544**

SENSITIVITY AND UNCERTAINTY ANALYSES FOR A SARS MODEL WITH TIME-VARYING INPUTS AND OUTPUTS

Robert G. McLeod

Department of Mathematics and Statistics, University of Winnipeg
Winnipeg, MB, Canada R3B 2E9

John F. Brewster

Department of Statistics, University of Manitoba
Winnipeg, MB, Canada R3T 2N2

Abba B. Gumel

Department of Mathematics, University of Manitoba
Winnipeg, MB, Canada R3T 2N2

Dean A. Slonowsky

Department of Mathematics, Malaspina University-College
Nanaimo, BC, Canada V9R 5S5

Abstract. This paper presents a statistical study of a deterministic model for the transmission dynamics and control of severe acute respiratory syndrome (SARS). The effect of the model parameters on the dynamics of the disease is analyzed using sensitivity and uncertainty analyses. The response (or output) of interest is the control reproduction number, which is an epidemiological threshold governing the persistence or elimination of SARS in a given population. The compartmental model includes parameters associated with control measures such as quarantine and isolation of asymptomatic and symptomatic individuals. One feature of our analysis is the incorporation of time-dependent functions into the model to reflect the progressive refinement of these SARS control measures over time. Consequently, the model contains continuous time-varying inputs and outputs. In this setting, sensitivity and uncertainty analytical techniques are used in order to analyze the impact of the uncertainty in the parameter estimates on the results obtained and to determine which parameters have the largest impact on driving the disease dynamics.

1. **Introduction.** A novel disease known as severe acute respiratory syndrome (SARS) was reported in March, 2003 by the World Health Organization (WHO) [31]. This respiratory disease, caused by a previously unknown coronavirus, SARS-CoV [6, 14, 18, 22, 32], spread to 32 countries and regions, causing 774 deaths and 8,096 infections globally [30]. The high mortality and morbidity associated with the virus, coupled with its rapid global spread, prompted a coordinated global effort spearheaded by WHO and aimed at determining effective control strategies for

2000 *Mathematics Subject Classification.* 92D30.

Key words and phrases. control reproduction number, epidemiological model, functional output, Latin hypercube sampling, partial rank correlation coefficients.

combatting the spread of SARS. Thankfully, these efforts resulted in the elimination of all cases of SARS by August 2003 [7, 30].

Numerous mathematical models have been designed and used to evaluate control strategies against SARS in some of the SARS-stricken regions (see, for instance, [5, 7, 9, 11, 12, 13, 21, 28, 29, 33]). These models, generally in the form of systems of deterministic or stochastic differential and difference equations, contain many parameters. The study of the dynamics of such a new emerging disease presents important challenges not only because of the uncertainty in the estimates of the model parameters, but also because control measures are gradually refined as more data (and further knowledge about the disease) become available.

This paper, which focuses on the mathematical model presented in [7], aims to investigate the effect of the uncertainty associated with the parameter estimates used in [7]. In this work we (i) extend the model in [7] by incorporating continuous time-dependent functions into the model to reflect the gradual refinement of control measures over time and (ii) apply sensitivity and uncertainty analysis (SUA) techniques to the resulting model containing continuous inputs and outputs.

It is known that the behaviour of nonlinear and multidimensional mathematical models can be explored using SUA (see [23] and the references therein). While an uncertainty analysis quantifies the variability in the outcome of the model attributable to the uncertainty in the values of the associated input parameters, a sensitivity analysis enables the determination of the most influential parameters driving a model.

In the context of disease epidemiology, SUA has been used (notably by Blower and co-workers [2, 3, 4, 24]) to gain insights into the transmission and control dynamics of many human diseases such as HIV and tuberculosis. For example, in [2], SUA was used to investigate a model for the evolution of drug-resistant HIV in San Francisco. This model featured two continuous time-varying outcome variables (prevalence and transmission of drug resistance). Our paper incorporates continuous time-varying input functions (Section 3) into the underlying mathematical model in [7], and we use SUA techniques similar to those in [2, 3, 4, 24] to assess the epidemiological significance of the input parameters, including those associated with the new functions that we introduce to model the gradual refinement of anti-SARS control measures.

In this paper, SUA techniques are used to identify the key epidemiological parameters affecting the dynamics (persistence or elimination) of SARS. Owing to the uncertainty in parameter estimation associated with a new emerging disease such as SARS (where some of the key biological and epidemiological features are not precisely known at the beginning of the epidemic), a detailed SUA is imperative to ascertain the effect of such uncertainties on the results obtained from associated mathematical models.

Unlike most epidemiological models, the modified model considered here involves time-varying, continuous, control parameters in addition to a time-dependent response. The time-varying control parameters are used to model the progressive refinement of quarantine and isolation measures for SARS-infected individuals. Furthermore, the model includes a time-varying component representing the gradual implementation of hygienic precautions by health workers and others in close contact with infected individuals in isolation. The existence of a time-dependent response implies that functional data is obtained as output. Functional data arise in many different fields, with the characteristic feature that the output consists

of (typically smooth) curves [19, 20]. In the SUA literature, however, little use is made of the functional analytic concepts described in [19] and [20]. Although the analytical techniques used in this paper do not fully exploit the functional nature of the data, they do provide a starting point and the motivation for future research on the development of SUA techniques for epidemiological models with functional output.

The paper is organized as follows. The underlying SARS transmission model is briefly described in Section 2. Section 3 presents time-dependent control strategies used to further refine the model of Section 2. SUA techniques employed in the analysis of the modified model are described in Section 4.

2. **Mathematical model.** The model proposed in [7], which subdivides a given SARS-affected region into six mutually exclusive subpopulations (susceptible (S), asymptomatically infected (E), quarantined (Q), symptomatic (I), isolated (J) and recovered (R) individuals), consists of the following differential equations:

$$\frac{dS}{dt} = \Pi - \frac{S(\beta I + \epsilon_E \beta E + \epsilon_Q \beta Q + \epsilon_J \beta J)}{N} - \mu S, \tag{1}$$

$$\frac{dE}{dt} = p + \frac{S(\beta I + \epsilon_E \beta E + \epsilon_Q \beta Q + \epsilon_J \beta J)}{N} - (\gamma_1 + \kappa_1 + \mu)E, \tag{2}$$

$$\frac{dQ}{dt} = \gamma_1 E - (\kappa_2 + \mu)Q, \tag{3}$$

$$\frac{dI}{dt} = \kappa_1 E - (\gamma_2 + \delta_1 + \sigma_1 + \mu)I, \tag{4}$$

$$\frac{dJ}{dt} = \gamma_2 I + \kappa_2 Q - (\sigma_2 + \delta_2 + \mu)J, \tag{5}$$

$$\frac{dR}{dt} = \sigma_1 I + \sigma_2 J - \mu R. \tag{6}$$

In (1)-(6), the total population at time t, denoted by $N(t)$, is given by $N(t) = S(t) + E(t) + Q(t) + I(t) + J(t) + R(t)$. The associated model parameters and variables are described in Tables 1 and 2. Since the above model monitors human populations, all parameters and state variables are assumed nonnegative for all t. For further details about the model and its associated parameters, the reader may refer to [7].

The model has a disease-free equilibrium (DFE) given by

$$(S^*, E^*, Q^*, I^*, J^*, R^*) = \left(\frac{\Pi}{\mu}, 0, 0, 0, 0, 0\right). \tag{7}$$

Following [7], let

$$R_c = \frac{\epsilon_E \beta}{D_1} + \frac{\beta \kappa_1}{D_1 D_2} + \frac{\epsilon_Q \beta \gamma_1}{D_1 D_4} + \frac{\epsilon_J \beta \kappa_1 \gamma_2}{D_1 D_2 D_3} + \frac{\epsilon_J \beta \gamma_1 \kappa_2}{D_1 D_3 D_4}, \tag{8}$$

with $D_1 = \gamma_1 + \kappa_1 + \mu$, $D_2 = \gamma_2 + \delta_1 + \sigma_1 + \mu$, $D_3 = \sigma_2 + \delta_2 + \mu$ and $D_4 = \kappa_2 + \mu$. By linearizing the model around the DFE with $p = 0$, the following result can be proven.

LEMMA 1. *The DFE, (7), of the model (1)-(6), is locally asymptotically stable if* $R_c < 1$ *and unstable if* $R_c > 1$.

The threshold quantity R_c is called the *control reproduction number* [1], which represents the average number of new infections generated by a single infective when SARS control measures are in place. Lemma 1 shows that introducing a

TABLE 1. Descriptions of State Variables and Time-Independent Parameters

Variable or Par.	Interpretation
β	Infectiousness and contact rate between a susceptible and symptomatic individual
κ_1	Rate of development of clinical symptoms in asymptomatic population
κ_2	Rate of development of clinical symptoms in quarantined class
σ_1	Rate of recovery in symptomatic class
σ_2	Rate of recovery in isolated class
δ_1	Disease induced death rate in symptomatic class
δ_2	Disease induced death rate in isolated class
μ	Natural death rate
ϵ_E	Modification parameter associated with infection from asymptomatic individual
ϵ_Q	Modification parameter associated with infection from quarantined individual
Π	Rate of inflow of individuals into a region or community
p	Rate of inflow of individuals that are infected asymptomatically
S	Subpopulation of susceptible (noninfected) individuals
E	Subpopulation of asymptomatically infected individuals (exhibiting no SARS symptoms)
Q	Subpopulation of quarantined asymptomatically infected individuals
I	Subpopulation of individuals with clinical symptoms of SARS
J	Subpopulation of isolated symptomatic individuals
R	Subpopulation of individuals who recovered from SARS

TABLE 2. Control-Related Parameters

Variable	Interpretation
γ_1	Quarantine rate (per day) of asymptomatic individuals
γ_2	Isolation rate of symptomatic individuals
ϵ_J	Modification parameter associated with infection from isolated individual

small number of infectives into the population will not lead to a major epidemic if $R_c < 1$ (i.e., in this case, SARS will be eliminated if $R_c < 1$). Similarly, SARS will persist in the population if $R_c > 1$. For a review of reproduction numbers, see [8].

2.1. **Parameters for control measures.** In the absence of a rapid diagnostic test, therapy or vaccine, SARS control measures were based on quarantine (of exposed individuals), isolation (of symptomatically infected individuals) and stringent hygienic precautions during isolation (prescribed for health care personnel). In the model (1)-(6), parameters corresponding to the health control measures (HCMs)—quarantine, isolation and hygienic precautions—are denoted by γ_1, γ_2 and ϵ_J, respectively (see Table 2). It should be noted that, in the model, individuals in quarantine are assumed to be asymptomatically infected.

In [7], γ_1 and γ_2 were set to 0 on the day (February 23, 2003) the index case was reported in the Greater Toronto Area (GTA) and switched to $\gamma_1 = 0.1$ and $\gamma_2 = 0.5$ a few weeks later (March 30, 2003), signifying the full implementation of the quarantine and isolation programs.

One key feature of the 2003 SARS outbreak was that, subsequent to the introduction of quarantine and isolation measures, a large number of nosocomial infections were reported. These infections were attributed to inadequate hygienic precautions taken by health care workers who came in contact with isolated infectives. The modification factor, ϵ_J, was introduced into the model in [7] to reflect the level of hygienic precautions undertaken during isolation. Perfect hygienic precautions would mean $\epsilon_J = 0$, implying that further SARS infections were not arising through contact with isolated individuals. The transmission coefficient, $\epsilon_J\beta$, associated with SARS transmission during isolation was larger before stringent hygienic measures were put in place. In [7], ϵ_J was set to 0.36 prior to April 30, 2003, after which ϵ_J was switched to 0.

Although γ_1, γ_2 and ϵ_J are modelled as discontinuous step functions in [7], as described above, such functions are somewhat simplistic in reflecting the progressive refinement of HCMs over time. Rather, it seems more plausible to model γ_1, γ_2 and ϵ_J as continuous, time-varying functions. In this manuscript we construct such input functions, and analyze the resulting continuous, time-varying, output functions.

3. **Development of time-varying control functions.** As mentioned in Section 2, it is assumed that the aforementioned SARS control measures were ineffective at the beginning of the epidemic, but were *progressively refined over time.* In contrast with modelling γ_1, γ_2 and ϵ_J via simple step-functions, as in [7], this paper introduces continuous, time-varying functions for better representing the gradual implementation of HCMs. Notationally, $\gamma_1(t), \gamma_2(t)$ and $\epsilon_J(t)$ are now time-dependent, and their functional forms are described in detail below.

As a starting point for constructing the time-varying control functions, consider the following cumulative distribution function, defined on $\Re$:

$$H_e(z) = \begin{cases} 0, & z < -1, \\ 0.5(1+z)^{1+e}, & -1 \le z < 0, \\ 1 - 0.5(1-z)^{1+e}, & 0 \le z < 1, \\ 1, & z \ge 1, \end{cases}$$

where $e \ge 0$. The function H_e is a standardized version of a control function, where the parameter e determines how quickly the anti-symmetric function H_e moves from its initial value of 0, at $z = -1$, to its final value of 1, at $z = 1$. To allow for the possibility of initial and final values other than 0 and 1 and for alternative ranges for the support of the distribution, the following continuous time-dependent function

$$h(t; a, b, c, d, e) = a + (b - a)H_e\Big(\frac{t - c}{d}\Big)$$

is used. The functional forms (with inflection point at $t = c$) for $\gamma_1(t), \gamma_2(t)$ and $\epsilon_J(t)$ are now defined by setting

$$\gamma_i(t) = h(t; a_i, b_i, (r_i + s_i)/2, (s_i - r_i)/2, e_i),$$

for $i = 1, 2$ and

$$\epsilon_J(t) = h(t; a_J, b_J, (2r_J + d_J)/2, d_J/2, e_J),$$

yielding

$$\gamma_1(t) = \begin{cases} a_1, & t < r_1, \\ a_1 + (b_1 - a_1)0.5\Big(1 + \Big(\frac{t-(r_1+s_1)/2}{(s_1-r_1)/2}\Big)\Big)^{1+e_1}, & r_1 \le t < (r_1+s_1)/2, \\ a_1 + (b_1 - a_1)\Big(1 - 0.5\Big(1 - \Big(\frac{t-(r_1+s_1)/2}{(s_1-r_1)/2}\Big)\Big)^{1+e_1}\Big), & (r_1+s_1)/2 \le t < s_1, \\ b_1, & t \ge s_1, \end{cases}$$

$$\gamma_2(t) = \begin{cases} a_2, & t < r_2, \\ a_2 + (b_2 - a_2)0.5\Big(1 + \Big(\frac{t-(r_2+s_2)/2}{(s_2-r_2)/2}\Big)\Big)^{1+e_2}, & r_2 \le t < (r_2+s_2)/2, \\ a_2 + (b_2 - a_2)\Big(1 - 0.5\Big(1 - \Big(\frac{t-(r_2+s_2)/2}{(s_2-r_2)/2}\Big)\Big)^{1+e_2}\Big), & (r_2+s_2)/2 \le t < s_2, \\ b_2, & t \ge s_2, \end{cases}$$

and

$$\epsilon_J(t) = \begin{cases} a_J, & t < r_J, \\ a_J + (b_J - a_J)0.5\Big(1 + \Big(\frac{t-(2r_J+d_J)/2}{d_J/2}\Big)\Big), & r_J \le t < (2r_J+d_J)/2, \\ a_J + (b_J - a_J)\Big(1 - 0.5\Big(1 - \Big(\frac{t-(2r_J+d_J)/2}{d_J/2}\Big)\Big)\Big), & (2r_J+d_J)/2 \le t \\ & < (r_J+d_J), \\ b_J, & t \ge s_J. \end{cases}$$

Although the functions above may appear somewhat complex at first glance, they are actually quite simple and easy to interpret. They represent a natural way of moving from an initial value of a to a final value of b in a continuous antisymmetric manner between times $t = r$ and $t = s$. The parameter e reflects the speed at which implementation of the relevant control measure takes place between times r and s. Other functional forms could have been used instead; in fact, any suitably parameterized cumulative distribution function for a continuous random variable on the interval $(-1, 1)$ could have been used in place of H_e. The function need not be antisymmetric. Moreover, the standardized function could be defined on an infinite range, such as $(0, \infty)$, with appropriate modifications being made to the definition of h. This would permit time-varying functions analogous to exponential decay to be used. However, it is thought that the functions used in this paper provide a suitable representation of the implementation of SARS control measures, while being flexible enough to permit a SUA to be performed on the model parameters.

3.1. **Parameters for the time-dependent functions.** Prior to implementation of quarantine, $\gamma_1(t) = a_1 = 0$. That is, no one is quarantined for $t < r_1$, where the parameter r_1 represents the time (number of days since onset of epidemic) at which health care professionals first introduce quarantine measures for asymptomatically-infected individuals. The parameter s_1 represents the number of days (since onset of epidemic) until quarantine is implemented throughout the region of interest. At $t = s_1$, the function $\gamma_1(t) = b_1$, the limiting (final) value for $\gamma_1(t)$. It is assumed that the maximum attainable quarantine rate is reached at time $t = s_1$. The parameter e_1 determines the "shape" of $\gamma_1(t)$ between days r_1 and s_1. For example, if $e_1 = 0$, then $\gamma_1(t)$ will be linear between days r_1 and s_1. Furthermore, $e_1 > 0$ implies that implementation of HCMs are slower near days r_1 and s_1, and faster near the inflection point, $(r_2 + s_2)/2$.

TABLE 3. The Time-Dependent Functions

Functions & Par.	Interpretation
$\gamma_1(t)$:	Quarantine rate (per day) of asymptomatic individuals
a_1	Nonpublic health-imposed quarantine (self-reporting) rate
b_1	Quarantine rate after quarantine HCMs are fully implemented
r_1	Time (days since onset of epidemic) at which quarantine HCMs are first introduced
s_1	Time (days since onset of epidemic) at which quarantine HCMs are fully implemented
e_1	Shape parameter for $\gamma_1(t)$ between r_1 and s_1
$\gamma_2(t)$:	Isolation rate of symptomatic individuals
a_2	Nonpublic health-imposed isolation (self-reporting) rate
b_2	Isolation rate after isolation HCMs are fully implemented
r_2	Time (days since onset of epidemic) at which isolation HCMs are first introduced
s_2	Time (days since onset of epidemic) at which isolation HCMs are fully implemented
e_2	Shape parameter for $\gamma_2(t)$ between r_2 and s_2
$\epsilon_J(t)$:	Infectiousness and contact rate between susceptible and individual in isolated class
a_J	Infectiousness and contact rate before hygienic precautions are first introduced
b_J	Infectiousness and contact rate after hygienic precautions are fully implemented
r_J	Time (days since onset of epidemic) at which proper hygienic precautions are introduced
d_J	Time (number of days) taken to fully implement proper hygienic precautions
e_J	Shape parameter for $\epsilon_J(t)$ between r_J and s_J

From a health policy standpoint, it is also useful to consider the reparametrization $d_1 = s_1 - r_1$, the number of days required to fully adhere to quarantine HCMs. An analysis (see Section 4) investigating the time required for the health-care system to respond completely and effectively to the SARS epidemic will shed light on how delays in implementation could significantly increase the number of SARS cases.

Table 4 provides ranges (and nominal values) of the parameters associated with the function $\gamma_1(t)$. While the parameter ranges were selected so that the SUA analysis could investigate a wide variety of plausible disease scenarios, the nominal values correspond to reasonable baseline values for the parameters based on the GTA estimates contained in [7]. The functional form for $\gamma_1(t)$ is depicted in Figure 1 using the nominal values of a_1, b_1, r_1, s_1 and e_1 (given in Table 4).

The parameters associated with the function $\gamma_2(t)$ are similarly defined (see Table 3), although several distinctions are noted below. First, before isolation measures are introduced ($t < r_2$), it is assumed that a small number of individuals may voluntarily "isolate" themselves at hospitals because of rapidly failing health.

TABLE 4. Ranges and Nominal Values for the Time-Dependent Functions

Functions & Parameters	Range	Nominal Values
$\gamma_1(t)$:		
a_1	Fixed at 0	0
b_1	[0.05, 0.2]	0.1
r_1	$[15 \leq r_2 \leq r_1 \leq 35]$	25
s_1	$[35 \leq s_2 \leq s_1 \leq 75]$	55
e_1	[0, 2]	1
$\gamma_2(t)$:		
a_2	[0, 0.2]	0.1
b_2	[0.4, 0.6]	0.5
r_2	See r_1	See r_1
s_2	See s_1	See s_1
e_2	[0,2]	1
$\epsilon_J(t)$:		
a_J	[0.3, 1]	0.36
b_J	Fixed at 0	0
r_J	$[r_2 + 10, r_2 + 20]$	40
d_J	[0, 14]	7
e_J	Fixed at 0	0

TABLE 5. Ranges and Nominal Values for the Time-Independent Parameters

Parameter	Range	Nominal Values
β	$[0, 0.6]$	0.2
κ_1	$[0.1 \leq \kappa_1 \leq \kappa_2 \leq 0.167]$	0.1
κ_2	See κ_1	0.125
σ_1	$[0.027 \leq \sigma_1 \leq \sigma_2 \leq 0.058]$	0.0337
σ_2	See σ_1	0.0386
δ_1	$[0.005 \leq \delta_2 \leq \delta_1 \leq 0.02]$	0.0079
δ_2	See δ_1	0.0068
μ	Fixed at 0.000034	
ϵ_E	Fixed at 0	
ϵ_Q	Fixed at 0	

This possibility is incorporated by letting a_2 vary between 0 and 0.2 (Table 4) so that $a_2 \geq a_1$. In line with [7], it is assumed that the isolation rate is greater than the quarantine rate so that $b_2 > b_1$. From the preceding discussion, it is reasonable to expect that control measures will be introduced and subsequently implemented sooner for symptomatic individuals than for asymptomatic individuals (so that $r_2 \leq r_1$ and $s_2 \leq s_1$).

The infectiousness and contact rates between a susceptible and a SARS-infected individual in the asymptomatic, quarantined and isolated classes are denoted by ϵ_E, ϵ_Q and ϵ_J, respectively. As in [7], we set $\epsilon_E = \epsilon_Q = 0$ since small values for these modification parameters yield similar simulation results. However, the infectiousness and contact rate between a susceptible and a SARS-infected individual in the isolated class is modelled as a function of time using $\epsilon_J(t)$. The modification

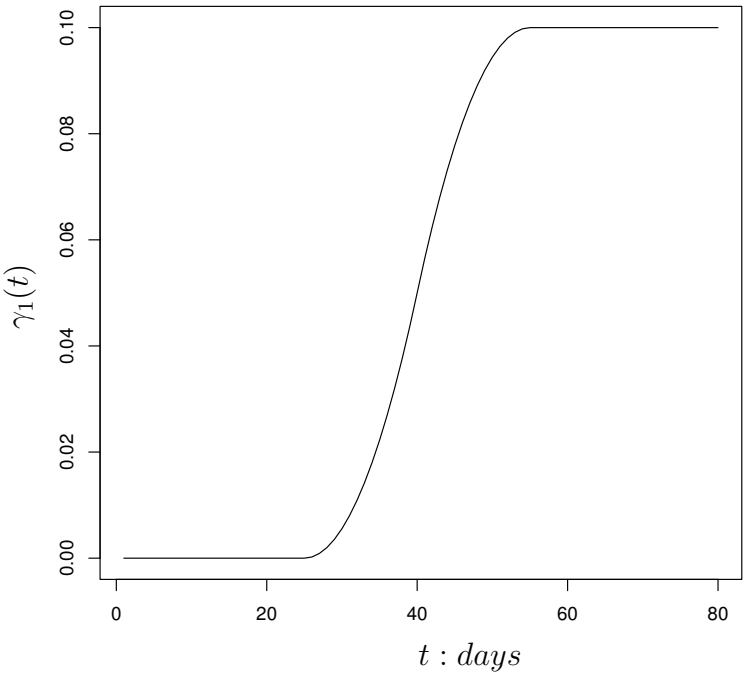

FIGURE 1. Functional form of $\gamma_1(t)$, the quarantine rate of asymptomatic individuals, with a_1, b_1, r_1, s_1 and e_1 at their nominal values

parameter, $\epsilon_J(t)$, adjusts β to reflect changes in the baseline SARS infectiousness and contact rate as hygienic precautions are gradually implemented by health care workers.

We assume that $\epsilon_J(t)$ is initially positive by setting $\epsilon_J(t) = a_J$ until $t = r_J$, the time at which proper hygienic precautions (gloves, face masks, etc.) are first introduced. When hygienic precautions are fully implemented (at time $t = d_J$), then $\epsilon_J(t) = b_J = 0$.

4. **SUA of the refined SARS model.** This section employs analytical tools from the field of SUA to identify key parameters in the refined SARS model, given by (1)-(6), with $\gamma_1(t), \gamma_2(t)$ and $\epsilon_J(t)$ as defined in Section 3. We begin the section by describing techniques for sampling the input parameter values from their proposed ranges (Tables 4 and 5). This is followed by application of uncertainty analysis techniques to the refined SARS model. An uncertainty analysis is conducted to quantify how the uncertainty in the choice of input parameter values produces variability in the response(s). The uncertainty analysis is followed by a sensitivity analysis to ascertain those parameters in the model which are most influential (this enables the ranking of input parameters in terms of their effect on the response).

It is worth stating that replacing the control parameters γ_1, γ_2 and ϵ_J in the autonomous model (1)-(6) with their respective time-dependent formulations from

Section 3 makes the model nonautonomous. Nonetheless, since the control reproduction number for the autonomous case (R_c) governs the persistence or effective control of SARS near the DFE, it is instructive to analyze the dynamics of this threshold when time-dependent functions are used. In other words, this study monitors, as output, the behavior of R_c as a function of time ($R_c(t)$).

Before assessing the effect of parameter uncertainty on the response, a methodology for selecting (sampling) input parameter values has to be chosen. Many sampling techniques are available to practitioners, but each must be judged in the light of model assumptions, resource availability and other practical considerations.

For the SARS model under consideration, a given sampling approach must ensure reasonable coverage of the high-dimensional parameter space while remaining parsimonious in terms of total sample (run) size. To accomplish this, we employ a sampling technique known as Latin hypercube sampling (LHS) [2, 3, 15, 23, 24, 25]. In terms of its space-filling qualities, LHS is typically superior to simple random sampling (SRS) in cases where many parameters are present in a model and limitations exist on the number of runs that are computationally practical. The superiority of LHS is particularly realized when the response of interest is a monotonic function of each of the input parameters.

LHS has been extended to include other criteria in the sample selection process to produce samples with additional desirable space-filling properties [16, 17, 25, 26, 27]. These refinements to LHS are not required here, because of the ease with which relatively large samples can be selected in this problem.

Parameters are treated as random variables in LHS. Thus, probability distributions must be assigned to each parameter prior to the selection of the parameter values. Our ensuing analysis assumes that the parameters are either independently uniformly distributed, pairwise uniform on constrained (triangular) regions, or conditionally specified. In the context of the refined SARS model, ranges for the parameters are provided in Tables 4 and 5. It should be noted that the parameters a_1, b_J, e_J, μ, ϵ_E and ϵ_Q are fixed. Using the preceding methodology, samples of size $n = 1,000$ and $n = 2,000$ were generated. Although the SUA in the subsequent sections will focus only on the results obtained for $n = 1,000$, the plots, analyses and conclusions were similar for the case with $n = 2,000$. As noted above, it was relatively easy to obtain a large sample in this problem, so it was possible to compare the results from different sample sizes. The sample size of $n = 1,000$ was chosen because the curves were smooth and the results were stable by that point. In general, the required sample size will depend on the number of parameters and the characteristics of the problem. However, it is of interest to note that [2, 3] also use $n = 1,000$ in their simulations.

4.1. **Uncertainty analysis.** For each of the 1,000 runs of the LHS, a "curve", $R_c(t)$, is generated as the response. A question that arises is how to conduct a SUA when the output has such functional characteristics. In our uncertainty analysis, we adopt a cross-sectional approach, except when analyzing the response t^* below. Although the cross-sectional approach does not fully exploit the functional analytic nature of the output, it will be shown that this approach leads to useful conclusions in this problem. This is largely because the curves of interest are monotone decreasing for the parameter combinations under consideration. The cross-sectional approach would not work nearly as well if the curves were more complex. The approach used here provides a starting point for conducting a SUA for a model with functional output and serves as a springboard for future research.

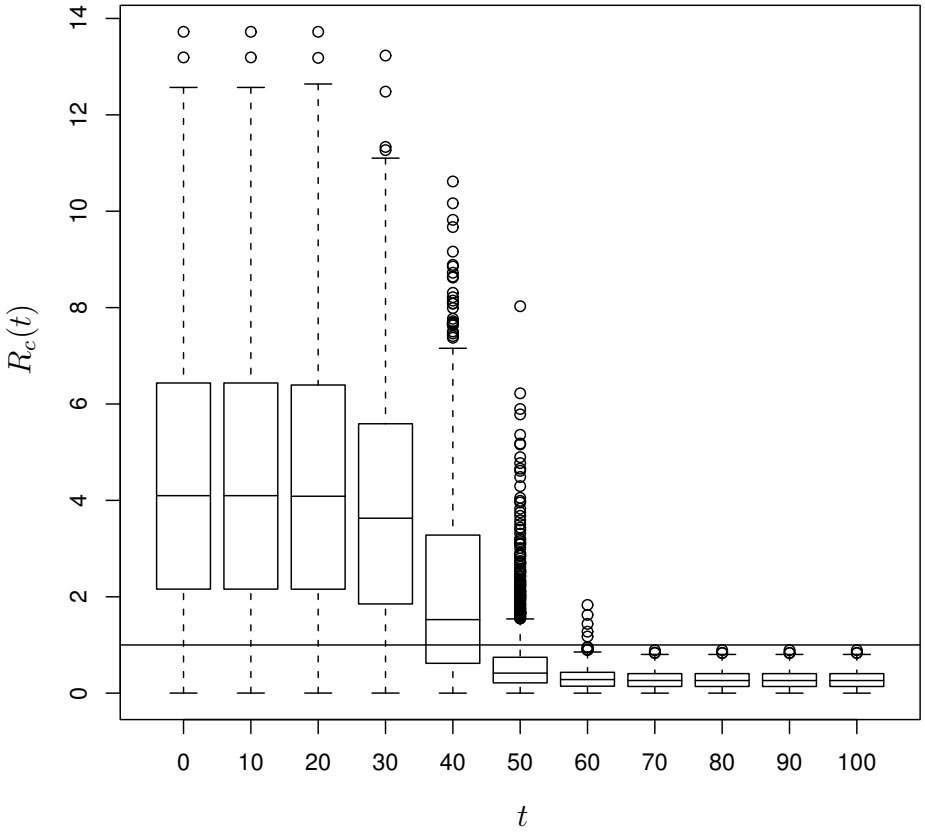

FIGURE 2. Control reproduction number, $R_c(t)$ vs. number of days since onset of epidemic

Figure 2 displays the boxplots of the response, $y = R_c(t)$, for days $t = 0, 10, \ldots, 100$. At a given day, each boxplot displays the $25^{\text{th}}(Q_1)$ and $75^{\text{th}}(Q_3)$ percentiles of $R_c(t)$. The 25^{th} and 75^{th} percentiles are denoted by the lower and upper horizontal lines on a box, respectively. The horizontal line within a box denotes the median value (50^{th} percentile) of $R_c(t)$. The "whiskers" protruding from each box extend to the most extreme values for $R_c(t)$, which are no more than $1.5(Q_3 - Q_1)$ away from the box. Any value for $R_c(t)$ plotted beyond the whiskers is classified as an outlier. Finally, the solid line depicts the line $R_c(t) = 1$. Although no theoretical analyses of the nonautonomous model are reported here, it is reasonable to infer that values of $R_c(t)$ less than one correspond to cases where initial SARS outbreaks are effectively controlled, and values greater than one correspond to cases where SARS will persist (in line with the theoretical results for the autonomous case given by Lemma 1).

The boxplots of $R_c(t)$ are monotonically decreasing over $t = 0, 10, \ldots, 100$. Most $R_c(t)$ curves become less than one at around 40 to 60 days after the onset of the epidemic, although some $R_c(t)$ values are less than one at $t = 0$. Figure 2 further demonstrates that there are no changes in the $R_c(t)$ curves between $t = 0$ and $t = 10$. Also, there is very little movement in these curves between $t = 10$ and $t = 20$. Recall that health control measures are not implemented until $t = 15$ (Table 4); therefore, changes in values for the time-dependent functions $(\gamma_1(t), \gamma_2(t)$ and $\epsilon_J(t))$ comprising $R_c(t)$ do not occur until after this time. Lastly, the presence of outliers in Figure 2 indicates that certain parameter configurations result in values of $R_c(t)$ that are markedly higher than the "typical" values inside of the boxes. Under these parameter configurations, SARS would persist for a longer period of time.

We now consider the distribution of the response, $y = t^*$, the first day at which $R_c(t) = 1$. Figure 3 presents a boxplot and histogram of t^*. The median number of days (since the onset of epidemic) until $R_c(t) = 1$ is just over 40. Aside from the values for which $t^* = 0$, the histogram exhibits a roughly symmetric distribution.

4.2. **Sensitivity analysis.** Sensitivity analysis employs quantitative methods for determining which parameters have the largest impact on a model's response variables. From the previous section, it should be recalled that the response variables are $R_c(t)$ at fixed time points (days) and t^*, the first day at which $R_c(t) = 1$.

Many sensitivity analytical techniques are available [23]; some of the more popular techniques include various graphical methods (scatterplots, cobweb plots), correlation measures (partial correlation, rank correlation), regression methods (stepwise regression, rank regression, nonparametric regression) and more advanced approaches such as
variance-based methods (sensitivity indices, total effect indices).

4.2.1. *Partial rank correlation coefficients.* In line with [2, 3, 4, 10, 23, 24], our sensitivity analysis begins with the calculation of partial rank correlation coefficients (PRCCs). This means that, in our case, the PRCCs must be calculated between each of the $k = 19$ nonconstant parameters and the responses $R_c(t)$ at each time t and t^*. Calculating PRCCs between inputs and a response is a useful exploratory technique for ascertaining the importance of individual parameters, or main effects. The attraction of PRCCs also lies in their computational simplicity and in their ability to parallel conclusions obtained by more advanced sensitivity procedures.

To calculate PRCCs, we first convert the input parameter values to their respective rank (1 to n) with a response. The reasons for using ranks in place of the actual parameter and response values are two-fold. First, unlike the actual measurements, the ranks for each parameter and output automatically have the same scale and range. More importantly, whereas the output ($R_c(t)$ or t^*) is monotone in each parameter, the relation between any particular parameter, x_i, and the output may be highly nonlinear. In this scenario, the usual partial correlation coefficient, being suited for assessing a linear relationship between a parameter and a response, may not properly reflect the strength of the influence of an x_i on the output. Once PRCCs have been calculated, parameters can be ranked in descending order of epidemiological importance, according to the magnitude of their PRCCs. Parameters having PRCCs approaching the bounds -1 or $+1$ signify a stronger impact on the output $(R_c(t))$.

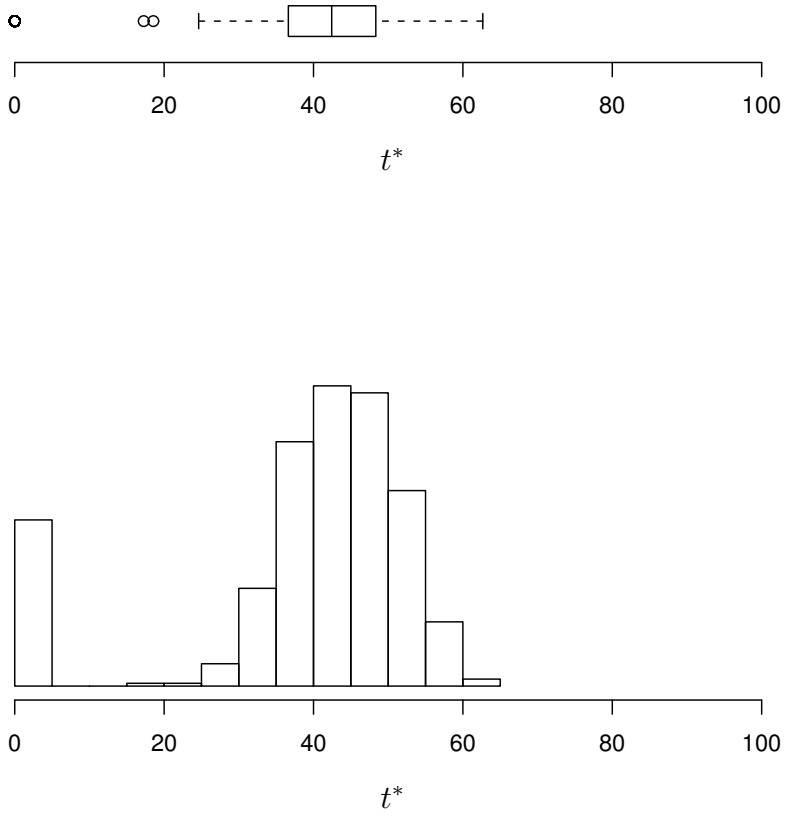

FIGURE 3. The distribution of t^*, the first day at which $R_c(t) = 1$

Note that, in this section, we consider $d_1 = r_1 - s_1$ and $d_2 = r_2 - s_2$ rather than s_1 and s_2, explicitly. As mentioned in Section 3.1, this reparametrization will assist in the interpretability of the model and the development of useful health policy strategies.

PRCC curves between each of the 19 nonconstant parameters (Tables 4 and 5) and $R_c(t)$ are plotted continuously as a function of time, t (Figure 4). (It is worth emphasizing that this approach is similar to that used in [2], in which PRCCs were calculated for different years, when modelling the transmission of drug-resistant HIV.) To reduce "clutter," we use separate graphs when plotting the PRCC curves for the time-independent parameters (Figure 4(d)) and the parameters corresponding with the time-dependent functions, $\gamma_1(t), \gamma_2(t)$ and $\epsilon_J(t)$ (Figures 4(a)-(c)).

Figure 4(d) shows that for all t, β has the largest positive PRCC of the time-independent parameters. This large PRCC for β implies that as the infectiousness and contact rate between a susceptible and symptomatic individual increases, so too will the length of time required before SARS is eliminated. Justification for

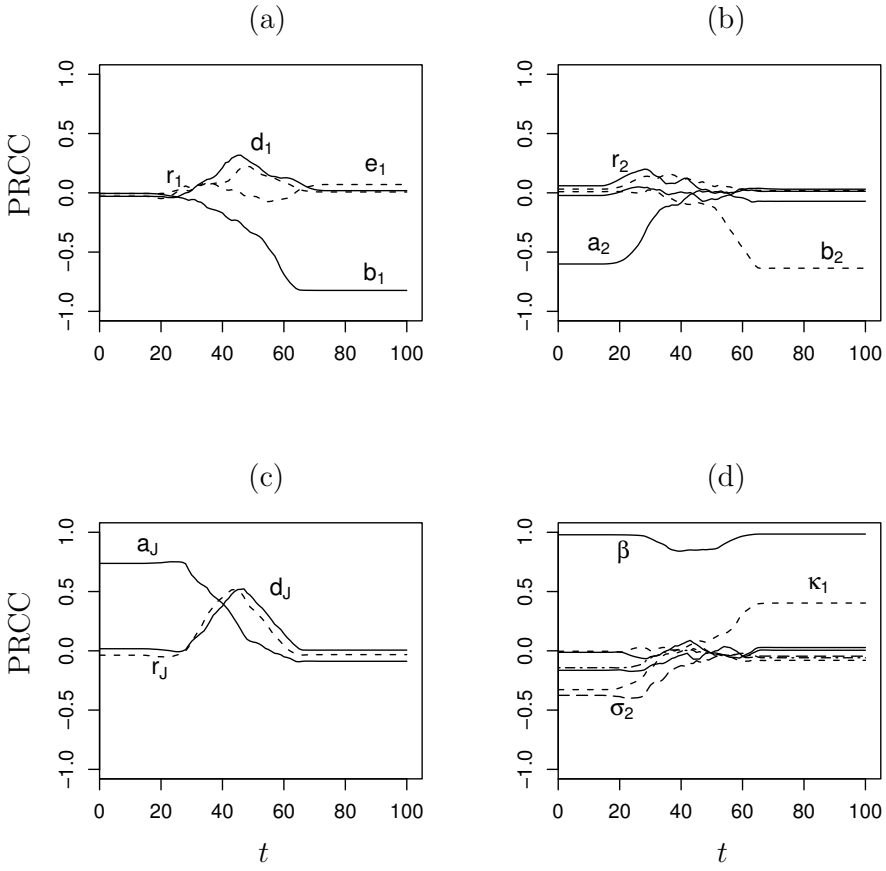

FIGURE 4. Partial rank correlation coefficients, over time, of the time-independent and time-dependent parameters with the control reproduction number, $R_c(t)$

such a strong relationship between β and $R_c(t)$ may also be obtained directly from the equation for $R_c(t)$ in (8), from which it is evident that β is (positively) linearly related to $R_c(t)$ (since β could be factored out from each numerator in (8)). Of the remaining time-independent parameters, the most influential are κ_1 (rate of development of clinical symptoms in the asymptomatically infected population) and σ_2 (rate of recovery in the isolated class). The parameter σ_2 has PRCCs of about -0.4 until (approximately) $t = 25$ days, at which point its correlation with $R_c(t)$ drifts toward zero. The parameter κ_1 has PRCCs of approximately 0.4 when $t > 60$ days. For $t > 40$ days, the PRCCs of all remaining time-independent parameters tend toward zero (suggesting their marginal significance in driving the disease dynamics).

For the 12 nonconstant parameters associated with $\gamma_1(t), \gamma_2(t)$ and $\epsilon_J(t)$, Figures 4(a)-(c) suggest three distinct stages in the transmission and control dynamics

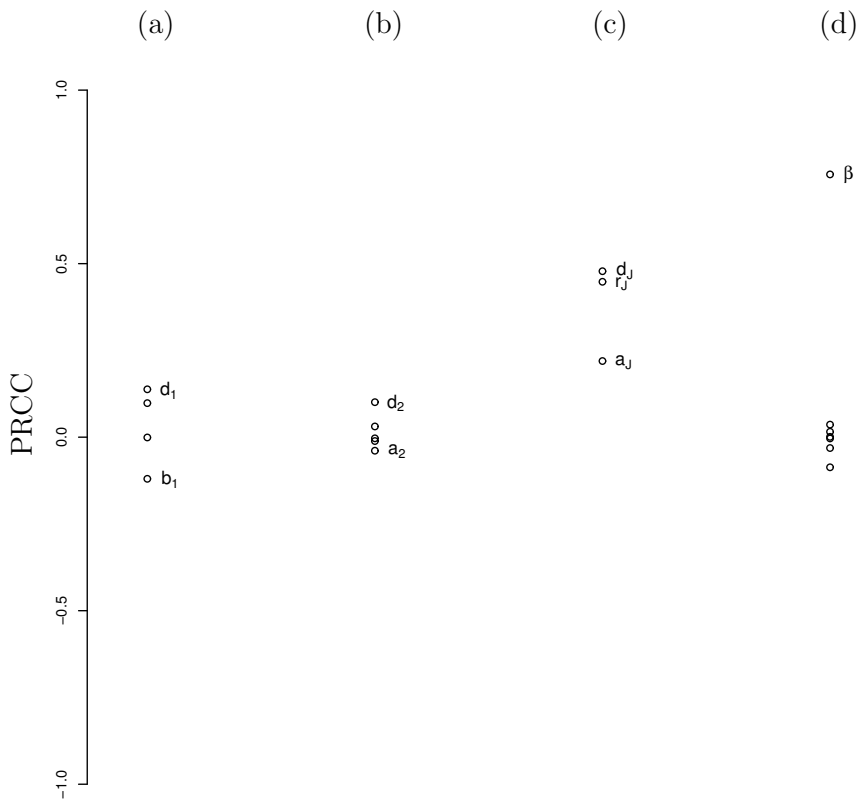

FIGURE 5. Partial rank correlation coefficients of the time-independent and time-dependent parameters with t^*, the first day at which $R_c(t) = 1$

of SARS. In the early stages of the outbreak (approximately 0 - 30 days), the two parameters (other than β) that most influence $R_c(t)$ are a_2, the rate of self-reporting (self-isolation) and a_J, the infectiousness of SARS prior to the implementation of hygienic precautions during isolation. In the intermediate stage (approximately 30 - 60 days), the influence of a_2 and a_J on $R_c(t)$ decreases. During this second stage, there is also a marked increase in the influence of d_1 (the number of days taken to fully implement quarantine HCMs) and d_J (the number of days needed to fully adhere to proper hygienic precautions) on $R_c(t)$. In the third and final stage (approximately 60 days and beyond), the influences of d_1 and d_J wane while the influence of b_1 (the asymptotic quarantine rate) and b_2 (the asymptotic isolation rate) become prominent.

Figure 5 displays the PRCCs of the time-independent and time-dependent parameters with t^*. The parameters most influential in determining the time at which $R_c(t) = 1$ are β, d_J and r_J. Although β is intrinsic to SARS, the parameters d_J and r_J can be controlled by health care professionals, and as suggested by Figure 5, an early and rapid implementation of stringent hygienic precautions will have a significant impact on the timely elimination of SARS.

4.2.2. *Contour plots of two-parameter interactions.* Although PRCCs are suitable for determining the effect of individual parameters on a response, they fail to provide insight regarding the effect of parameter interactions on the model output. As a means for investigating interactions amongst parameters, we construct two-dimensional contour plots of (x_i, x_j) for $R_c(t)$ and t^*. Clearly, an investigation of all ${}_{19}C_2 = 171$ possible two-parameter interactions for each response would be formidable. Instead, rank regression models [23, 25] can be used to identify which two-parameter interactions to investigate. In rank regression analysis one replaces the original data with their corresponding ranks to form first- and second-order regression models. Those interactions having the largest (statistically significant) impact on $R_c(t)$ and t^* can be identified and plotted.

Figures 6(a) and (b) display contour plots of $R_c(40)$ for the two-parameter interactions βd_1 and βd_2, both of which were found to have a significant impact on $R_c(40)$. Given that we have no control over β, these two-parameter interactions suggest that, in the presence of a large β, it is imperative that health care personnel implement quarantine and isolation as quickly as possible, once such measures are deemed necessary.

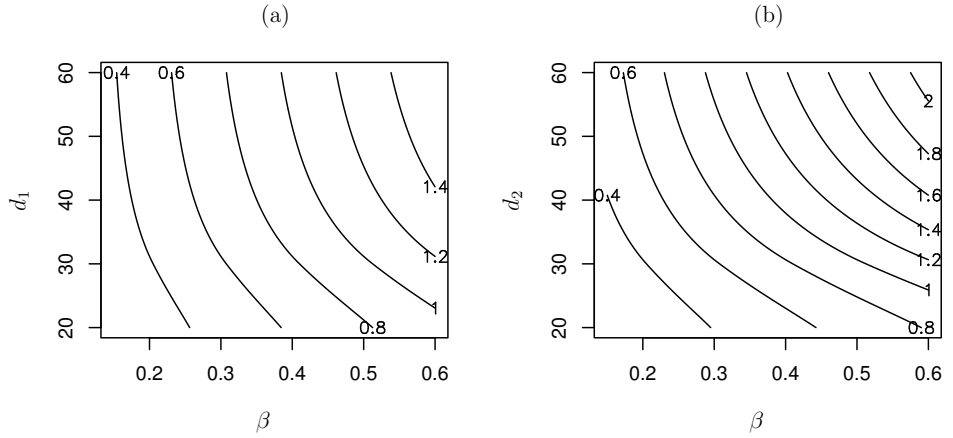

FIGURE 6. Contour plot of $R_c(40)$ by (a) β and d_1 and (b) β and d_2

5. **Conclusions.** In this paper we modify a deterministic model for the transmission dynamics of SARS to include the progressive refinement of anti-SARS control measures. This is accomplished by introducing monotone, continuous, time-dependent functions that mimic the introduction and subsequent implementation of quarantine, isolation and hygienic precautions. Consequently, the model contains time-varying inputs and functional output. SUA techniques are applied to determine those parameters having the largest effect on the disease dynamics, as represented by $R_c(t)$.

Our analysis demonstrates the existence of three distinct stages in the evolution of SARS transmission dynamics where, other than the transmission rate (β), (i) in stage 1 (0 - 30 days of the epidemic), the self-isolation rate (a_2) and the infectiousness and contact rate prior to the implementation of hygienic precautions (a_J) are

the most critical parameters in determining the fate of the epidemic; (ii) in stage 2 (30 - 60 days of the epidemic), the number of days taken to fully implement quarantine (d_1), isolation (d_2) and hygienic precautions (d_J) are the most influential; (iii) in stage 3 (after 60 days), the maximum attainable rates of quarantine (b_1) and isolation (b_2) are the most critical parameters.

It is hoped that the conclusions drawn from this study will enhance our understanding of SARS and that the manner in which we have modelled the implementation of control measures will prove useful in other disease scenarios.

Acknowledgments. This work was supported in part by the Mathematics of Information Technology and Complex Systems (MITACS) of Canada, the Office of the Chief Scientist, Health Canada, and the Manitoba Centres of Excellence Fund (MCEF). Three of the authors (J.F.B., A.B.G. and D.A.S.) acknowledge, with thanks, the support of the Natural Sciences and Engineering Research Council (NSERC) of Canada. The authors are also grateful to Professor J. Wu (York University) and members of his MITACS infectious disease modelling team and to Dr. W. Cuff (National Microbiology Laboratory, Winnipeg) for many useful discussions. The authors are grateful to the two anonymous reviewers for their constructive comments, which have improved the paper.

REFERENCES

[1] R.M. Anderson and R.M. May, "Infectious Diseases of Humans," Oxford University Press, London, 1991.

[2] S.M. Blower, A.N. Aschenbach, H.B. Gershengorn and J.O. Kahn, *Predicting the unpredictable: Transmission of drug-resistant HIV*, Nature Med. (9) 7 (2001), 1016-1020.

[3] S.M. Blower and H. Dowlatabadi, *Sensitivity and uncertainty analysis of complex models of disease transmission: An HIV model, as an example*, Internat. Stat. Rev. 62 (1994), 229-243.

[4] S.M. Blower, D. Hartel, H. Dowlatabadi, R.M. Anderson and R.M. May, *Drugs, sex and HIV: A mathematical model for New York City*, Phil. Trans. R. Soc. Lond. B 321 (1991), 171-187.

[5] G. Chowell, P.W. Fenimore, M.A. Castillo-Garsow and C. Castillo-Chavez, *SARS outbreaks in Ontario, Hong Kong and Singapore: The role of diagnosis and isolation as a control mechanism*, J. Theoret. Biol. 224 (2003), 1-8.

[6] C. Drosten (and 24 others), *Identification of a novel coronavirus in patients with severe acute respiratory syndrome*, N. Engl. J. Med. 348 (2003), 1967-1976.

[7] A.B. Gumel (and 11 others), *Modelling control strategies for controlling SARS outbreaks*, Proc. R. Soc. Lond. B. 271 (2004), 2223-2232.

[8] J.M. Heffernan, R.J. Smith, L.M. Wahl, *Review. Perspectives on the basic reproductive ratio*, J. R. Soc. Interface 2 (2005), 281-293.

[9] Y.H. Hsieh, C.W.S. Chen, S.-B. Hsu, *SARS outbreak, Taiwan, 2003*, Emerg. Infect. Dis. 10 (2004), 201-206.

[10] M. Kendall and A. Stewart, "The Advanced Theory of Statistics. Volume II.," Hafner Publishing Company, New York, 1979.

[11] N. Lee (and 13 others), *A major outbreak of severe acute respiratory syndrome in Hong Kong*, N. Engl. J. Med. 348 (2003), 1986-1994.

[12] M. Lipsitch (and 11 others), *Transmission dynamics and control of severe acute respiratory syndrome*, Science 300 (2003), 1966-1970.

[13] J.O. Lloyd-Smith, A.P. Galvani, W.M. Getz, *Curtailing transmission of severe acute respiratory syndrome within a community and its hospital*, Proc. R. Soc. Lond. B. 270 (2003), 1979-1989.

[14] M.A. Marra (and 57 others), *The genome sequence of the SARS-associated coronavirus*, Science 300 (2003), 1399-1404.

[15] M.D. McKay, R.J. Beckman and W.J. Conover, *A comparison of three methods of selecting values of input variables in the analysis of output from a computer code*, Technometrics 21 (1979), 239-245.

[16] M.D. Morris and T.J. Mitchell, *Exploratory designs for computational experiments*, J. Statist. Plann. Inference 43 (1995), 381-402.
[17] K. Palmer and K.-L. Tsui, *A minimum bias Latin hypercube design*, IEEE Transactions 33 (2001), 793-808.
[18] J.S.M. Peiris (and 15 others), *Coronavirus as a possible cause of severe acute respiratory syndrome*, Lancet 361 (2003), 1767-1772.
[19] J.O. Ramsay and B.W. Silverman, "Functional Data Analysis," Springer-Verlag, New York, 1997.
[20] J.O. Ramsay and B.W. Silverman, "Applied Functional Data Analysis: Methods and Case Studies," Springer-Verlag, New York, 2002.
[21] S. Riley (and 19 others), *Transmission dynamics of etiological agent of SARS in Hong Kong: The impact of public health interventions*, Science 300 (2003), 1961-1966.
[22] P.A. Rota (and 34 others), *Characterization of a novel coronavirus associated with severe acute respirtory syndrome*, Science 300 (2003), 1394-1399.
[23] A. Saltelli, K. Chan and E.M. Scott, "Sensitivity Analysis," John Wiley & Sons, Ltd., England, 2000.
[24] M.A. Sanchez and S.M. Blower, *Uncertainty and sensitivity analysis of the basic reproductive rate: Tuberculosis as an example*, Am. J. Epidemiol. 145 (1997), 1127-1137.
[25] T.J. Santner, B.J. Williams and W.I. Notz, "The Design and Analysis of Computer Experiments," Springer-Verlag, New York, 2003.
[26] B. Tang, *Orthogonal array-based Latin hypercubes*, J. Amer. Statist. Assoc. 88 (1993), 1392-1397.
[27] B. Tang, *Selecting Latin hypercubes using correlation criteria*, Statist. Sinica 8 (1998), 965-978.
[28] W. Wang and S. Ruan, *Simulating the SARS outbreak in Beijing with limited data*, J. Theoret. Biol. 227 (2004), 369-379.
[29] G.F. Webb, M.J. Blaser, H. Zhu, S. Ardal and J. Wu, *Critical role of nosocomial transmission in the Toronto SARS outbreak*, Math. Biosci. Engng. 1 (2004), 1-13.
[30] WHO. *Communicable disease surveillance and response*, [Accessed April, 2005] Available from: URL: http://www.who.int/csr/ sars/country/table2004_04_21/en/
[31] WHO. *China's latest SARS outbreak has been contained, but biosafety issues remain—update 7*, [Accessed May, 2004] Available from: URL: http://www.who.int/csr/don/2004_05_18a/en/
[32] WHO. *Coronavirus never before seen in humans is the cause of SARS*, [Accessed April, 2003] Available from: URL: http://www.who.int/mediacentre/release/2003/pr31/en/
[33] Y. Zhou, Z. Ma and F. Brauer, *A discrete epidemic model for SARS transmission and control in China*, Math. Comput. Model. 40 (2004), 1491-1506.

Received on April 26, 2005. Accepted on February 10, 2006.

E-mail address: r.mcleod@uwinnipeg.ca
E-mail address: john_brewster@umanitoba.ca
E-mail address: gumelab@cc.umanitoba.ca
E-mail address: slonowskd@mala.bc.ca